Journal of Applied Fluid Mechanics, Vol. 6, No. 3, pp. 453-463, 2013.
Available online at www.jafmonline.net, ISSN 1735-3572, EISSN 1735-3645.

Evaluation of Eddy Viscosity Models in Predicting Free-Stream Turbulence Penetration

M. Kahrom[1†] and A. Shokrgozar[2]

[1,2] *Mechanical Engineering Department, Ferdowsi University of Mashhad, Mashhad, Iran*
†*Corresponding Author Email: mohsen.kahrom@yahoo.co.uk*

(Received February 11, 2012; accepted May 21, 2012)

ABSTRACT

Turbulence schemes have long been developed and examined for their accuracy and stability in a variety of environments. While many industrial flows are highly turbulent, models have rarely been tested to explore whether their accuracy withstands such augmented free-stream turbulence intensity or declines to an erroneous solution. In the present study, the turbulence intensity of an air flow stream, moving parallel to a flat plate is augmented by the means of locating a grid screen at a point at which $Re_x=2.5\times10^5$ and the effect on the flow and the near-wall boundary is studied. At this cross section, the turbulence intensity is augmented from 0.4% to 6.6% to flow downstream. Wind tunnel measurements provide reference bases to validate the numerical results for velocity fluctuations in the main stream and at the near-wall. Numerically, four of the most popular turbulence models are examined, namely the one-equation Spalart-Almaras, the two equation Standard $k-\varepsilon$, the two equation Shear Stress Transport $k-\omega$ and the anisotropy multi equation Reynolds Stress Models (RSM). The resulting solutions for the domain are compared to experimental measurements and then the results are discussed. The conclusion is made that, despite the accuracy that these turbulence models are believed to have, even for some difficult flow field, they fail to handle high intensity turbulence flows. Turbulence models provide a better approach in experiments when the turbulence intensity is at about 2% and/or when the Reynolds number is high.

Keywords: Free stream turbulence, Turbulence intensity, Turbulence models, Turbulence penetration

NOMENCLATURE

Nomenclature should be in alphabetic order (A – Z) and Greek letters should follow after Latin letters in alphabetic order (α β ..)

C_{ij}	convection terms
$C_{\varepsilon 1}$	constant
$C_{\varepsilon 2}$	constant
$C_{\varepsilon 3}$	constant
C_{b2}	constant=0.662
C_{v1}	constant = 7.1
$D_{T,ij}$	turbulence diffusion
$D_{L,ij}$	molecular diffusion
DNS	Direct Numerical Simulation
EVM	Eddy-Viscosity Model
F_{ij}	production by System Rotation
G_k	effect of buoyancy on turbulence kinetic energy
U_i	i component of the velocity vector
U'	abbreviation for $\overline{u'^2}$ in the figures
u_τ	friction Velocity, $(\tau_w/\rho_w)^{1/2}$
u^+	u/u_τ
u'	fluctuating part of the velocity component
u_τ	shear Velocity
y^+	$y\,u_\tau/\nu_w$
x	distance from the leading edge
x_j	distance in the j direction
$\alpha_k, \alpha_\varepsilon$	ratios of effective to molecular viscosity in k and ε equations
ε	dissipation Rate
ϕ_{ij}	pressure Strain
γ	a dissipation variable, e.g.: ε, ω
μ	molecular viscosity

G_v ,Y_υ $S_{\tilde{\upsilon}}$	functions defined in the Spalart-Allmaras equation
HRN	High Reynolds Number
k	turbulence kinetic energy per unit mass
LES	Large Eddy Simulation
LRN	Low Reynolds Number
P_{ij}	stress Production
RNG	Re-Normalization Group theory
RSM	Reynolds Stress Model
SST	Shear Stress Transport model
S_k	source term for the k equation/ Mean rate of the stress tensor
T_i	turbulence intensity of flow
u_i	averaged stream velocity in the i direction
μ_t	turbulence eddy viscosity
$\mu_{effec\ k}$	effective viscosity in the k equation
$\mu_{effec\ \varepsilon}$	effective viscosity in ε equation
σ_k , σ_ε	constants for effective viscosity in the k and ε equations
υ	kinematic viscosity
$\tilde{\upsilon}$	Modeled quantity in the Spalart-Allmaras turbulence model
ζ	a dummy variable

1. INTRODUCTION

Flows in engineering applications are mostly three-dimensional, unsteady, highly chaotic and turbulent and span over a wide range of lengths and time scales. One measure of unsteadiness is the turbulence intensity which causes apparent shear stresses. In high intensity turbulent flows, such as those streaming through turbo-machinery blade rows or flowing through burners, the turbulence intensity is reported to be as high as 5 to 25%, (2004). This order of intensity disrupts the downstream flow field, penetrates into the boundary layer and modifies the shear layer structure. This issue has not yet been addressed in classical developments of turbulence modeling and so elaborate modeling techniques still seem to be in demand.

Another example of the complexity of such a flow field, which has recently received great attention in flow modeling, is the effect of free stream turbulence on the onset of the transitional boundary layer, Jungho (2004), Antonis (2003) and Mark (2004). Frequently, when high turbulence intensity flows through turbo-machinery blade rows or other cases of promoted boundary layers, a bypass transition occurs by which the laminar boundary layer abruptly turns turbulent. For transitional boundary layers, attempts have been made, through experimental data, to establish empirical correlations between free-stream turbulence intensity and transitional point Reynolds numbers, John (2004), Robert and Henningson (1999) and Rumsey and Spalart (2009). Though very helpful, this application is limited. When considering all of these cases, a general question arises as to how reliable the present turbulence models are for treating such a complex viscous flow field.
While, the numerical techniques are of great help in predicting flow developments, many of these models are based on some simplifications and assumptions. In general, the numerical modeling of turbulence is based on the Navier-Stokes (N-S) equations that can be classified into two categories: 1) Direct Numerical Simulations, namely the DNS models and 2) all other models which are based on the understanding of the physics of turbulence, i.e. the way flow develops and then the modeling of its fluctuations.

In many numerical techniques, in order to arrive at the final solution to cover a particular case of fluid flow, the turbulence convection, its generation, dissipation and diffusion are all modeled by large scale grids and a correlation is applied to determine the coefficients of these equations. Frequently, some simplification of the modeling is imposed, such as assuming isotropy and homogeneity for the flow field. Amongst these numerical techniques, simplifications to DNS models are minor, Schaffrath *et al.* (2007). However, the DNS technique is, in most cases, impracticable as LES and DES models are very elaborate and expensive for engineering calculations. What remains as an option are the Eddy-Viscosity Models (EVM) which is the most widely used turbulence models by engineers and research workers. Despite the attraction these models hold for engineers, rarely their ability to predict the turbulence penetration into the flow field, as well as into the boundary layers, been explored. This, in fact, is the main task of present research work, Xia (2011).

Interaction between free-stream turbulence and boundary layer turbulence is mainly driven by the wall normal fluctuation component of velocity, v'. By interaction with the near wall's tangential velocity fluctuation, u', an increased shear-stress $u'v'$ is caused which might enhance the skin friction or the heat transfer. Consequently a large amount of FST is damped. However, the desired behavior can only be achieved if this mechanism is suitably captured by the turbulence model.

In this paper, special attention is drawn to the ability of different Boussinesq models to imitate the important processes associated with the interaction of the free-stream turbulence, flow and boundary layer turbulence capabilities of the most widely used Eddy-Viscosity Models, together with RSM, in predicting the turbulence penetration into a flow field over a flat plate. This subject has never been studied to shed light for researchers and engineers working with intense turbulent flows.

For this study, the well known FLUENT code is selected as a code holding a wide spread attraction in

the area of industrial design which has been validated in many academic research evaluations. The authors of the present work have found over 500 ISI papers, published after 2005, which were based on FLUENT numerical evaluations while employing EVMs, Colella *et al.* (2011), Sohn and Reshotko (1991) and Spalart and Allmaras (1994), which makes the code suitable for evaluation in flows with augmented turbulence intensity. The case of a flat plate is chosen for the present study as it is simple and common to many engineering problems and one expects to achieve the most accurate results for this geometry. The numerical results are compared to similar experimental data of a wind tunnel measurement, Schelechting (2000). This paper is aimed at those engineers and researchers dealing with flows of high turbulence intensity, with the intention of advising them of the limits of the availability of Eddy-Viscosity Models.

2. FLOW FIELD DESCRIPTION

Physical domain was previously employed for experimental measurements in a wind tunnel by Sohn and Reshotko (1991). The study was conducted on a flow of air parallel to a flat plate at zero pressure gradients. The main stream flows with a constant velocity of $V = 33.3\ m/s$. As a result, laminar, transitional and turbulent boundary layers form. In the experimental setup, at $x = 12.5$ centimeters from the leading edge at which $\mathrm{Re}_x = 2.5\times10^5$, a grid screen is placed to impose a desired turbulence intensity into the air stream, Fig. 1.

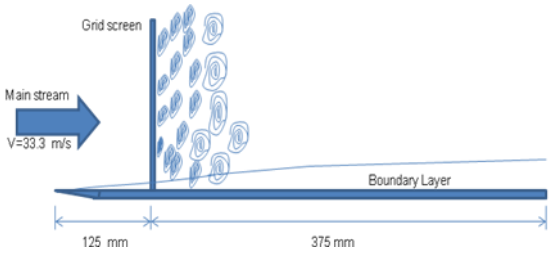

Fig. 1. Overall view of physical domain

To generate each of the turbulence intensities, a particular grid size screen must be located, Jungho (2004). Table 1 shows laboratory grid numberings and the expected turbulence intensity to be generated right after the screen.

Table 1 Equivalent turbulence intensity for each of the mesh sizing

Grid No.	0	0.5	1	2	3	4
Ti	0.004	0.008	0.011	0.026	0.056	0.066

In the numerical study, each grid screen is meant by its equivalent turbulence kinetic energy. Relations are:

$$k = \tfrac{1}{2}\left(\overline{u'^2 + v'^2 + w'^2}\right), \tag{1}$$

While:

$$Ti = \sqrt{\tfrac{1}{3}(\overline{u'^2} + \overline{v'^2} + \overline{w'^2})}/U_\infty \tag{2}$$

Then:

$$Ti = \frac{1}{U_\infty}\sqrt{\frac{2}{3}k} \tag{3}$$

In a wind tunnel, flow is isotropic at some distance behind the screen, Davidson (2003). For an isotropic flow, the average fluctuation of velocity is the same in all three coordinate directions i.e.:

$$\overline{\hat{u}^2} = \overline{\hat{v}^2} = \overline{\hat{w}^2} \tag{4}$$

In this case, the longitudinal velocity alone can be used as a measure of turbulence intensity. Thus:

$$T_i = \frac{\sqrt{\overline{\hat{u}^2}}}{U_\infty} \tag{5}$$

Thereafter, the equivalent turbulence intensity for each grid screen is:

$$Grid\ indication\,[0,\ 0.5,\ 1,\ 2,\ 3,\ 4] = k[0.027,\ 0.11,\ 0.2,\ 1.13,\ 5.22,\ 7.26] \tag{6}$$

In the present numerical study, the same physics of flow in the wind tunnel is followed. As in the wind tunnel, at $x = 12.5\ cm$, a grid mesh pushes the desired amount of turbulence into the flow field. In this paper, turbulence models of different orientations are employed in order to study how successful each model is in predicting turbulence penetration into the main field as well as into a turbulent boundary layer.

.

3. TURBULENCE MODEL AND GOVERNING EQUATIONS

The flow field is assumed to be steady, two dimensional incompressible and turbulent. The velocity components and pressure are governed by equations of continuity and momentum:

$$\frac{\partial U_i}{\partial x_i} = 0 \tag{7}$$

$$\frac{\partial U_i U_j}{\partial x_j} = -\frac{\partial p}{\partial x_i} + \frac{1}{\mathrm{Re}}\frac{\partial^2 U_i}{\partial x_j^2} \tag{8}$$

Amongst many turbulence models, some of the most popular are selected for evaluation. As a general trend, for all turbulence models, flow variables are decomposed into one average and one fluctuating part. If the fluctuating part is directly employed to estimate the mass and momentum transfer, the model is categorized as a Direct Numerical Simulation, namely the DNS method. If the average of fluctuations is used to define an apparent viscosity (υ_t), the model is recognized as one of the Bosinesque turbulence models. Most Bosinesque hypotheses-based models employ the isotropy assumption and are referred to as Eddy-

Viscosity Models (EVM). However, there are Reynolds Stress Models, in which the velocity fluctuations are used to predict apparent shear stresses, thus avoiding the isotropy assumption.

The obvious choice for one equation EVM is the famous Spalart-Allmaras model, Hussaini and Lumley (1996). This model solves a transport equation for a viscosity-like variable from which turbulence viscosity is the result. The Spalart-Allmaras model is said to be economical and accurate for attached wall-bounded flows and reliable for mild separation and the recirculation zone, Hussaini and Lumley (1996). Therefore it is an attractive model for external flows and aerodynamic purposes. The turbulence viscosity in this model is determined from:

$$\mu_t = \rho \tilde{\upsilon} \frac{\chi^3}{\chi^3 + C_{\upsilon 1}^3} \tag{9}$$

Where:

$$\chi = \frac{\tilde{\upsilon}}{\upsilon}$$

which is to be cast into Eq. (2):

$$\frac{\partial}{\partial t}(\rho \tilde{\upsilon}) + \frac{\partial}{\partial x_i}(\rho \tilde{\upsilon} u_i) = G_\upsilon + \frac{1}{\sigma_{\tilde{\upsilon}}}\left[\frac{\partial}{\partial x_j}\left((\mu + \rho \tilde{\upsilon})\frac{\partial \tilde{\upsilon}}{\partial x_j}\right) + C_{b2}\,\rho\left(\frac{\partial \tilde{\upsilon}}{\partial x_j}\right)^2\right] - Y_\upsilon + S_{\tilde{\upsilon}} \tag{10}$$

Other variables are defined in the nomenclature. Another selected EVM, which is widely used in engineering estimations, is the standard $k-\varepsilon$ model. The high Reynolds number version of this model uses the law of the wall to the estimate velocity profile near the wall. This model employs many less grid points and is economical for engineering studies. Simple implementation, stability, easily convergence and the reliable prediction of many engineering flows are the main advantages of this scheme. However, the disadvantages associated with it are poor prediction for rotating flows, questionable accuracy in strong separation, axis-symmetric jets and fully developed flows in non-circular ducts.

In Eddy Viscosity Models, by some modifications to its coefficients, the k equation is mainly common to all two-equation turbulence models and is always assumed to be, Davidson (2003), Stefes and Femholz (2004) and Zhang):

$$\frac{\partial}{\partial t}(\rho k) + \frac{\partial}{\partial x_i}(\rho k u_i) = \frac{\partial}{\partial x_j}\left(\mu_{effect\ k}\frac{\partial k}{\partial x_j}\right) + G_k + S_k + [terms\ added\ to\ k\ equ.] \tag{11}$$

The term in brackets is defined differently for various models and shall be defined for each model in the nomenclature.

For $k-\varepsilon$ models, the turbulence viscosity is assumed to be $\mu_t = \rho \zeta \frac{k^2}{\varepsilon}$. Separately, in $k-\omega$ models, it is defined as:

$$\mu_t = \rho \zeta \frac{k}{\omega} \tag{12}$$

An extra equation is then needed to close the two-equation models for locally isotropic flow fields. In general terms, this equation is represented as, Davidson (2003), Hussaini and Lumley (1996), Stefes and Femholz(2004), and Zhang":

$$\frac{\partial}{\partial t}(\rho \gamma) + \frac{\partial}{\partial x_i}(\rho \gamma u_i) = \frac{\partial}{\partial x_j}\left(\mu_{effect\ \varepsilon}\frac{\partial \gamma}{\partial x_j}\right) + S_\gamma + [terms\ added\ to\ \gamma\ equ.] \tag{13}$$

For Standard $k-\varepsilon$ models, assumptions are made as follows:

$$\zeta = C_\mu = 0.09 \quad Const. \qquad \gamma = \varepsilon$$
$$\mu_{effect\ K} = \mu + \frac{\mu_t}{\sigma_K}$$
$$\mu_{effect\ \varepsilon} = \mu + \frac{\mu_t}{\sigma_\varepsilon} \tag{14}$$
$$added\ terms\ to\ k\ equ. = G_b - \rho\varepsilon - Y_M$$

and:

$$added\ terms\ to\ \gamma\ equ. = C_{1\varepsilon}\frac{\varepsilon}{K}(G_K + C_{3\varepsilon} G_b) - C_{2\varepsilon}\,\rho\frac{\varepsilon^2}{K} \tag{15}$$

To end with two-equations EVM's, we employ the Menter`s Shear Stress Transport $k-\omega$ model, Xia (2011). This method combines the best of the two $k-\varepsilon$ and LRN $k-\omega$ models. In the inner parts of the boundary layer, down to the sublayer and wall, the SST employs the LRN $k-\omega$ model, thus gaining the benefits of the excellent near wall estimation of this model. As it approaches the main stream, the SST model gradually switches to HRN $k-\varepsilon$ to avoid the sensitivity of the $k-\omega$ model when competing with surrounding boundaries. These all together, the model is merited for its favorable performance in adverse pressure gradients and flows with separation.

For the SST $k-\omega$ model, some parameters read again, Davidson (2003), Zhang":

$$\zeta = \frac{1}{\max\left[\frac{1}{\alpha^*}, \frac{\sqrt{2\Omega_{ij}\Omega_{ij}}\,F_2}{a_1 \omega}\right]}, \tag{16}$$

$$F_2 = \tanh\left(\max\left[\frac{2\sqrt{k}}{0.09\,\omega\, y}, \frac{500\,\mu}{\rho\, y^2\, \omega} \right] \right)^2 ,$$

$$a_1 = 0.31 \qquad \gamma = \omega \tag{17}$$

Ω is the mean value of the rotational speed tensor and α^* is defined according to these Eq. (18):

$$\zeta_{L.R.N.} = \alpha^* = \alpha_\infty^* = \left(\frac{0.024 + \frac{\rho k}{6\mu\omega}}{1 + \frac{\rho k}{6\mu\omega}} \right) \tag{18}$$

$$\gamma = \omega$$
$$\zeta_{H.R.N} = \alpha^* = \alpha_\infty^* = 1 \tag{19}$$

$$\mu_{effect\ K} = \mu + \frac{\mu_t}{\sigma_K}$$
$$\mu_{effect\ \varepsilon} = \mu + \frac{\mu_t}{\sigma_\omega} \tag{20}$$

The added terms in the k equation, in brackets, are:

$$added\ terms\ to\ \gamma\ equation = G_\omega - Y_\omega + D_\omega \tag{21}$$

Very different from EVMs is the Reynolds Stress Model (RSM). This model avoids using the Boussinesq assumption and instead derives a transport equation for the stress tensor from the Navier-Stockes equations. This is why RSMs are frequently referred to as second-moment closure models, Stefes (2004). Resulting equations contain terms that need to be modeled. In 3-D flows, six equations have to be solved for stress terms $\overline{u'^2}, \overline{v'^2}, \overline{w'^2}, \overline{u'v'}, \overline{u'w'}, \overline{w'v'}$ together with an extra dissipation equation. Considering the three components of N-S equations and one for continuity, there is a total of ten equations, Dividson (2003).
The mathematical description of the model is elaborate and so avoided in this paper is. Interested readers may refer to, Hussaini and Lumley (1996) and Davidson (2003). The stress component equations read as:

$$\frac{\partial}{\partial t}\left(\rho \overline{u_i' u_j'} \right) + C_{ij} = D_{T,ij} + D_{L,ij} + P_{ij} + G_{ij} + \phi_{ij} + \varepsilon_{ij} + F_{ij} + S_{user} \tag{22}$$

For two-dimensional flows, coefficients $C_{ij}, D_{L,ij}, P_{ij}$ & F_{ij} are as defined in the nomenclature. However, the terms:

$$D_{T,ij}\ ,\ G_{ij}\ ,\ \phi_{ij} \text{ and } \varepsilon_{ij} \tag{23}$$

need to be modeled to close the stress equation. For two-dimensional domains, there are five equations to solve plus momentum and continuity equations.
Amongst the highlighted advantages of two-equation models, in comparison to RSM, one can say they are simple due to the isotropy assumption, stable and also short in CPU time consumption. On the other hand, RSMs are said to have the advantage of being accurate in curved geometries and vortex generating flows, Stefes and Femholz (2004).
Though RSMs are useful for all geometries as well as for curved walls, swirling flows and accelerating/retarding, they have the disadvantage of not being only complex and difficult to implement but also elaborate and time-consuming technique, Stefes and Femholz (2004).
Despite their reported advantages and disadvantages, all of the models discussed can be evaluated for how well and accurate they predict turbulence penetration into the main flow as well as into the boundary layers.
The zero equation, Large Eddy Simulation (LES), and Direct Numerical Simulation (DNS), are not addressed in this paper. In any case due to technical limitations, they are less common as applications used by engineers today.

4. NUMERICAL RESULT AND DISCUSSION

The Figs. 2- 5 compare the numerical results of turbulence models with the wind tunnel measure values of turbulence intensity along the flow field. For turbulence intensity as high as 6.6%, all models predict a decay of kinetic energy by about a 15% error in comparison to the experiment. However, numerical errors between the models themselves are within 3% along the free stream. For $T_i < 2\%$, turbulence intensity remains unchanged along the free-stream as these numerical results show.

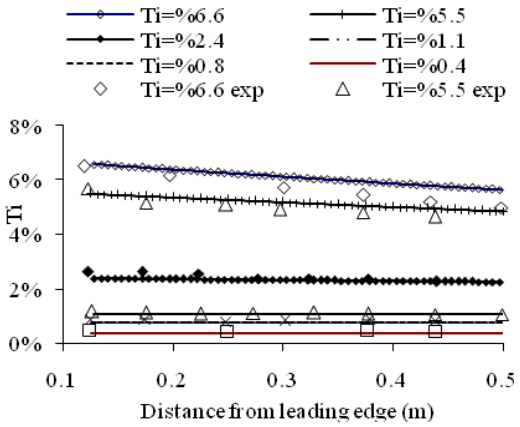

Fig. 2. Spalart-Almaras model predicting turbulence penetration into the main flow

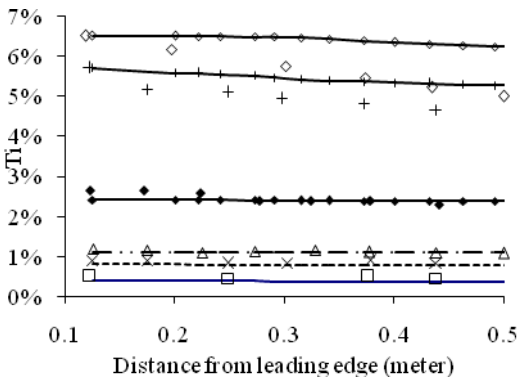

Fig. 3. Standard $k-\varepsilon$ model predicting turbulence penetration into the main flow

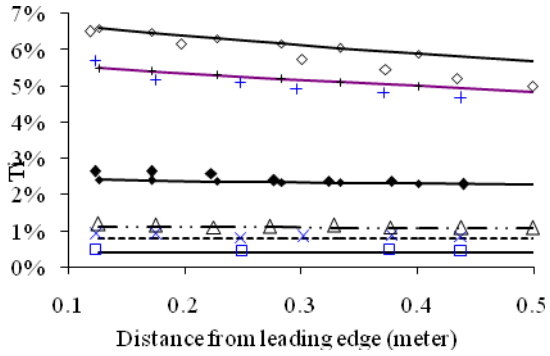

Fig. 4. SST $k-\omega$ model predicting turbulence penetration into the main flow

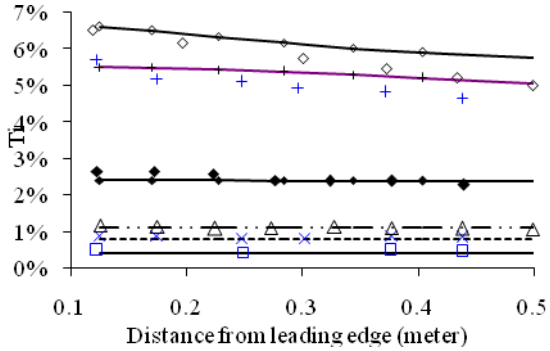

Fig. 5. RSM predicting turbulence penetration into the main flow

In short wall bounded flows, such as those in turbo machinery blade rows and heat exchangers, transitional boundary layers are one of the concerns of the flow field when arriving at a final solution. Transitional boundary layers are difficult to model, Wissink and Rodi (2011), and generally the case is simplified by approximating an extension to the turbulent boundary layer, Biau *et al.* (2007) and Rumsey and Spalart (2009). While this approximation has less effect on flows developing over long walls, it provides a poor solution for short length boundaries. In the present work, as the turbulence intensity is artificially augmented, the transitional process is assumed to be entailed by a turbulent boundary layer and the results are then compared to the experiments.

Two cases are selected for comparison. The first case features the medium turbulence intensity in the experiments, i.e. $T_i = 1.13\%$. The other case is $T_i = 5.22\%$ which delegates one of the high turbulence intensities. Figures 6 to 9 and Figs. 14 to 17 are plotted for the case of low turbulence intensity, $T_i = 1.13\%$. Figures 10 to 13 and Figs. 18 to 20 present the results of high turbulence intensity, $T_i = 5.22\%$. Note that curves for the experimental measurements of both turbulence intensities are repeatedly drawn in both groups of dependent figures. However, for all cases, the numerical results of each model differ considerably from the other models.

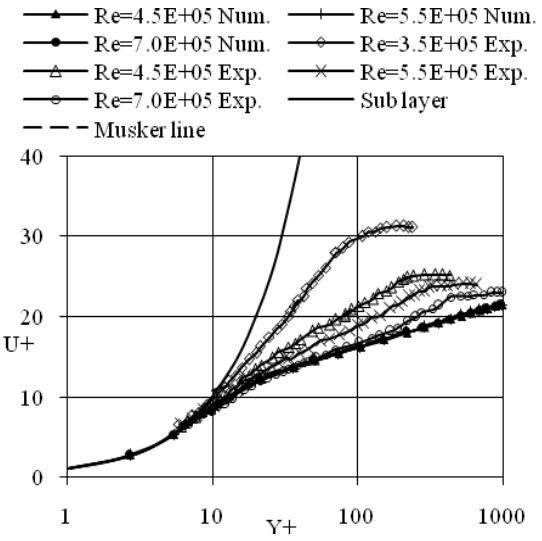

Fig. 6. Spalart-Almaras model predicting the near-wall velocity profile for various low main flow turbulence intensities compared to wind tunnel measurements, $T_i = 1.13\%$

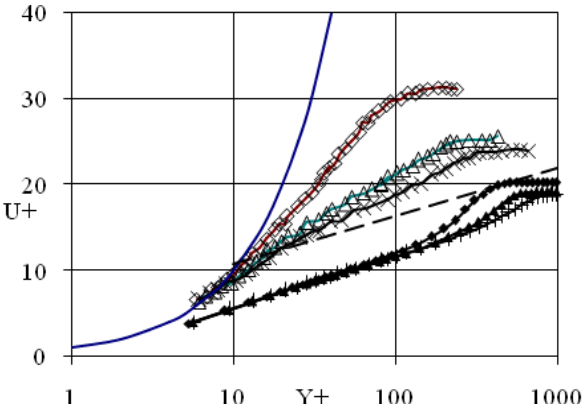

Fig. 7. Standard $k-\varepsilon$ model predicting the near-wall velocity profile for various low main flow turbulence intensities compared to wind tunnel measurements, $T_i = 1.13\%$

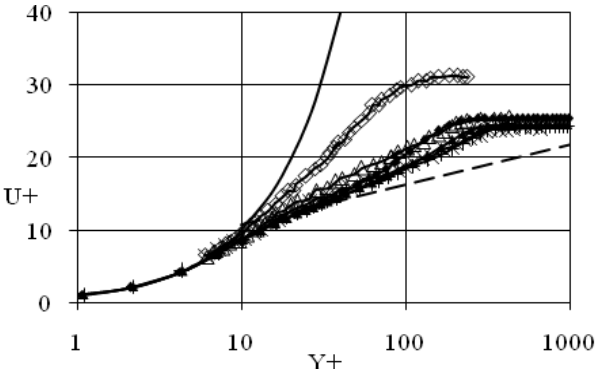

Fig. 8. SST $k-\omega$ model predicting near-wall velocity profile for various low main flow turbulence intensities compared to wind tunnel measurements, $T_i = 1.13\%$

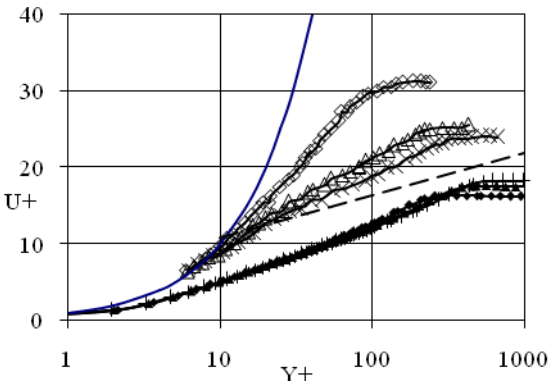

Fig. 9. RSM model predicting near-wall velocity profile for various low main flow turbulence intensities compared to wind tunnel measurements, $T_i = 1.13\%$

For low turbulence intensity, U^+ profiles are distinctly diverted from the experimental results. Figures 6 to 9 show the variations of U^+ at different stations along the flat plate. By increasing the values of T_i in the main stream, U^+ profiles at different stations approach each other, but for some models they are still far from the experimental results (Figs. 10 to 13). Indeed this study`s numerical schemes predict U^+ about an 85% error compared to the experiments at distances $20 < y^+ < 200$ from the flat plate (Figs. 6, 7 and 9.

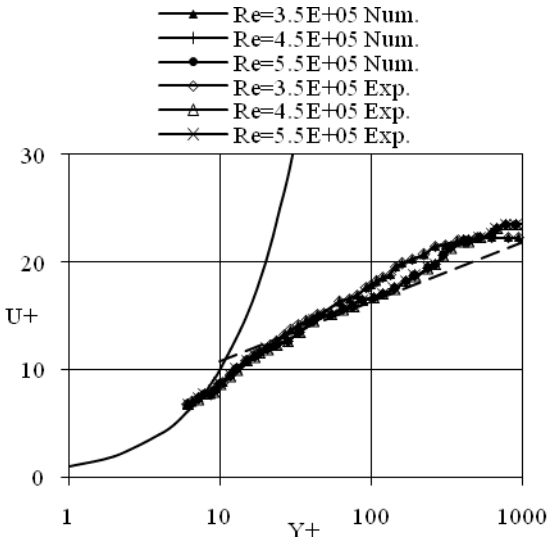

Fig. 10. Spalart-Almaras model predicting the near-wall velocity profile for various high main flow turbulence intensities compared to wind tunnel measurements, $T_i = 5.22\%$

For the high turbulence of the main flow, $T_i = 5.22\%$, Figures 10 and 12 present much better results. These figures show that higher turbulence intensity produces numerical results closer to measurements. In higherT_i, the results of the numerical schemes better approach those of the experiments, but the standard $k-\varepsilon$ and RSM models, still remain far away from those of the experiments and Musker line, Yang and Abdalla (2009). However amongst the numerical schemes, the Spalart-Almaras and SST $k-\omega$ models are nearer to the experiments (Figs. 10 and 12).

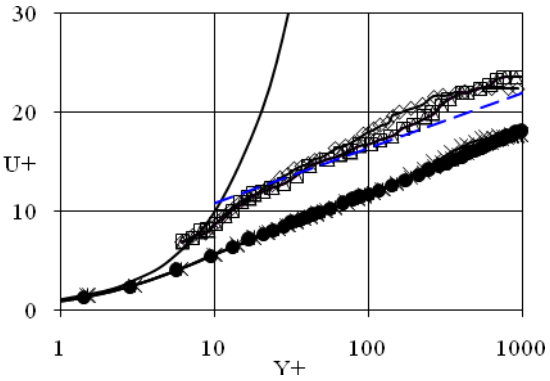

Fig. 11. Standard $k-\varepsilon$ model predicting the near-wall velocity profile for various high main flow turbulence intensities compared to wind tunnel measurements, $T_i = 5.22\%$

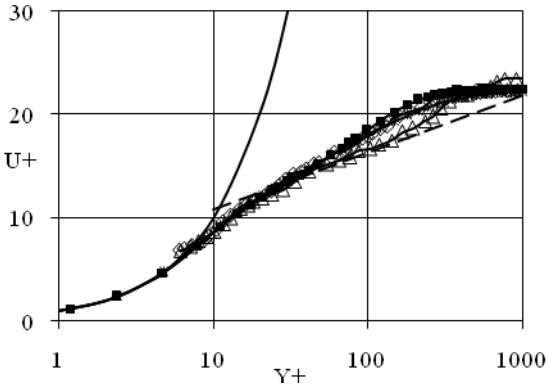

Fig. 12. SST $k-\omega$ model predicting the near-wall velocity profile for various high main flow turbulence intensities compared to wind tunnel measurements, $T_i = 5.22\%$

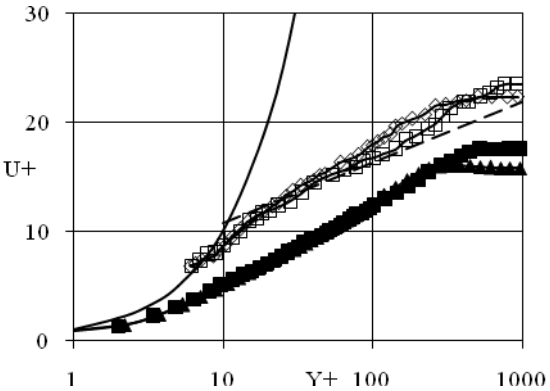

Fig. 13. RSM predicting the near-wall velocity profile for various high main flow turbulence intensities compared to wind tunnel measurements, $T_i = 5.22\%$

The variation of $\sqrt{u'^2}/u_\tau$ in the boundary layer is highly dependent on the free-stream turbulence intensity. At the low Reynolds numbers, $T_i = 1.13\%$, experimental

results show that a maximum value of $\sqrt{\overline{u'^2}}/u_\tau = 0.75$ appears at $y^+ \approx 20$, after which its value declines to a constant value extending to a free-stream turbulence intensity at the edge of the boundary layer. By moving further downstream, with the higher Re_x, the maximum value of the curve, expands over the range of $20 \leq y^+ \leq 120$ (Fig. 14).

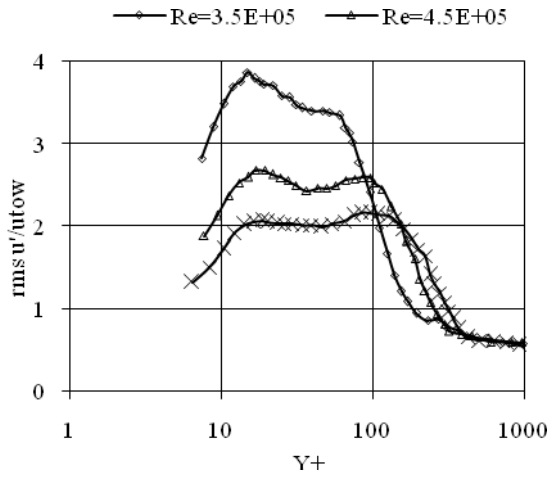

Fig. 14. Wind tunnel measurements at different Reynolds numbers along a flat plate for the low main flow turbulence intensity, $T_i = 1.13\%$

In the experimental results, by increasing Re_x and FSTI, the variation of $\sqrt{\overline{u'^2}}/u_\tau$ in the boundary layer builds up two maximum points. The first one appears at about $16.5 < y^+ < 35$ and the second one in between $70 < y^+ < 110$ from the plate (Fig. 18).

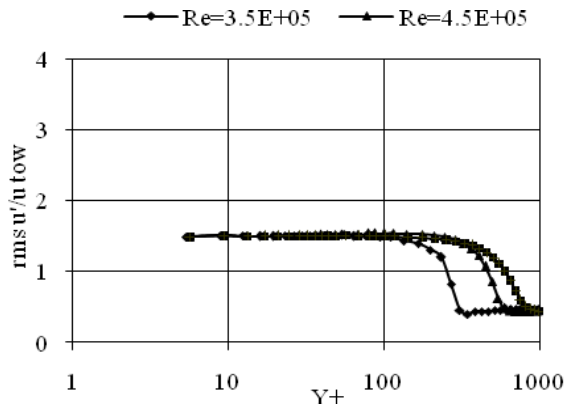

Fig. 15. Variation of $\sqrt{\overline{u'^2}}/u_\tau$ at different Reynolds numbers along a flat plate for the low main flow turbulence intensity, $T_i = 1.13\%$, predicted by $k-\varepsilon$ turbulence model

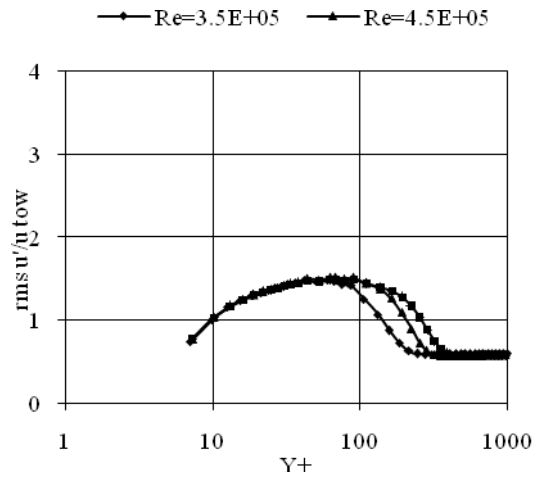

Fig. 16. Variation of $\sqrt{\overline{u'^2}}/u_\tau$ at different Reynolds numbers along a flat plate for the low main flow turbulence intensity, $T_i = 1.13\%$, predicted by the SST $k-\omega$ turbulence model

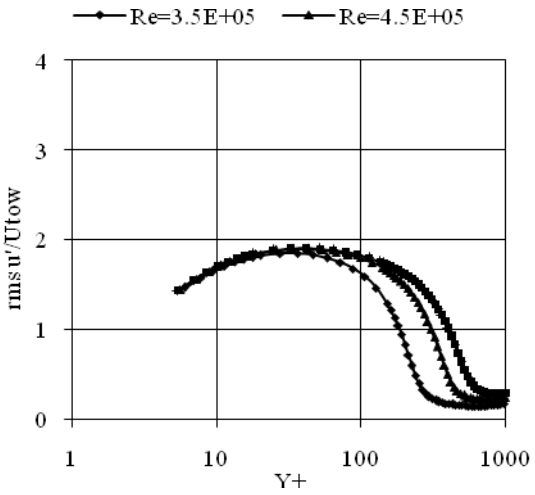

Fig. 17. Variation of $\sqrt{\overline{u'^2}}/u_\tau$ at different Reynolds numbers along a flat plate the for low main flow turbulence intensity, $T_i = \%1.13$, predicted by the RSM turbulence model

Unlike the experimental results, all turbulence models have a wide range of nearly constant values of $1.25 \leq \sqrt{\overline{u'^2}}/u_\tau \leq 1.5$, in between $10 < y^+ \approx 300$ measured from the wall. A dissimilarity exists in both the quality and quantities of $\sqrt{\overline{u'^2}}/u_\tau$ when compared to the experiments. As a general trend, $\sqrt{\overline{u'^2}}/u_\tau$, for all turbulence schemes, grows to a nearly constant value at about $y^+ \approx 10$. Thereafter, it remains nearly constant all the way through $10 < y^+ \approx 300$. This behavior of $\sqrt{\overline{u'^2}}/u_\tau$ is shown in Figs. 15, 18, 19 and 20 for all models and for almost all FSTIs, at all Re_x s under consideration.

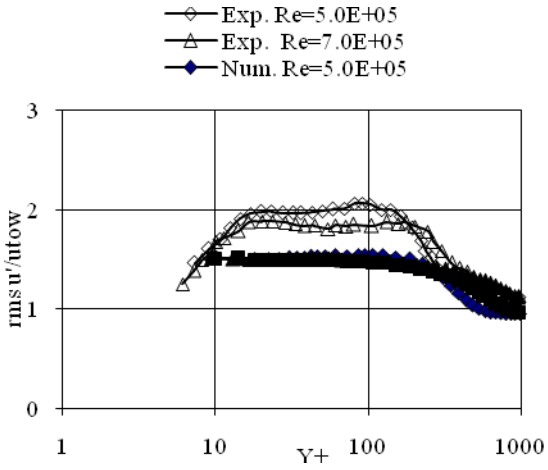

Fig. 18. The results of the standard $k-\varepsilon$ model, for the variation of $\sqrt{\overline{u^2}}/u_\tau$ at different Reynolds numbers along a flat plate, is compared to wind tunnel measurements for the high main flow turbulence intensity, $T_i = 5.22\%$

The maximum value of $\sqrt{\overline{u^2}}/u_\tau$, for all cases never exceeds 1.5 and at this amount, it spans over a large part of the boundary layer thicknesses. Worst is the standard $k-\varepsilon$ model as shown in Fig. 15 and Fig. 18 and the SST $k-\omega$ model in Fig. 16. Yet again, when approaching the free-stream at $y^+ > 500$, the results are pushed by the model to approach the free-stream turbulence intensity. The same is true for the near-wall results at which $\sqrt{\overline{u^2}}/u_\tau$ approaches zero.

This general observation differs slightly for some models. A better qualitative approach for $\sqrt{\overline{u^2}}/u_\tau$ is achieved by the RSM model for the high values of $T_i = 5.22\%$. However, even in this case, the order of error is at about 50%.

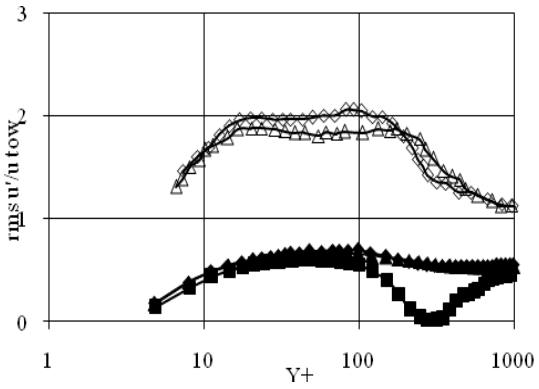

Fig. 19. The results of the SST $k-\omega$ model, for the variation of $\sqrt{\overline{u^2}}/u_\tau$ at different Reynolds numbers along a flat plate, is compared to wind tunnel measurements for the high main flow turbulence intensity, $T_i = 5.22\%$

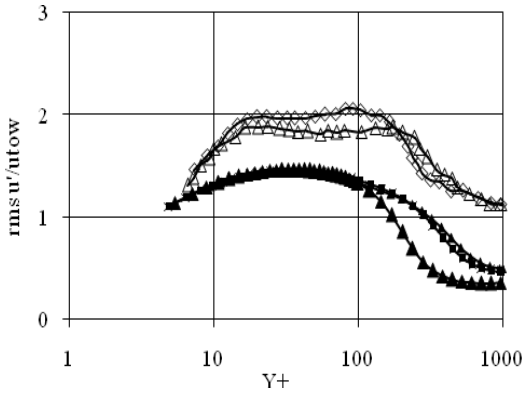

Fig. 20. The results of the RSM model, for the variation of $\sqrt{\overline{u^2}}/u_\tau$ at different Reynolds numbers along a flat plate, is compared to wind tunnel measurements for the high main flow turbulence intensity, $T_i = 5.22\%$

5. SUMMARY AND CONCLUSION

The performance of turbulence models in predicting the turbulence level along a free-stream over a flat plate and the effect of its penetration into the nearby boundary layer are explored. In the boundary layer, the variation of u^+ and the Reynolds stresses are computed and compared to those of the measurements in the wind tunnel.

Four of the most attractive turbulence models, namely the one-equation Spalart-Almaras, the two-equation high Reynolds number $-\varepsilon$, the two-equation low Reynolds number $SST\ k-\omega$ and the multi-equations non-isotropic RSM are considered. These models delegate a wide range of Eddy-Viscosity Models.

Two different turbulence levels are intended. One is the medium turbulence intensity level of 1.13% which appears in untreated flows such as pipe flows and most external flows. The second level is the high turbulence intensity level of about 6.6% which delegates most industrial flows involving energy transfer, such as those moving through turbomachineries and heat exchangers. Two different locations downstream from the turbulence generator screen are selected for evaluation. The first location is positioned at $Re_x = 4.5E{+}05$, which is close to the laminar portion of the boundary layer. The other location is assumed at $Re_x = 7.5E+05$ away from the transition point. Arrangements and configurations for wind tunnel measurements and the numerical evaluations are identical.

Numerical results show that for high turbulence intensities along the distance $x = 0.1\ m$ to $x = 0.5\ m$, the rate of dissipation of Ti is slower than that measured in the wind tunnel. The Spalart –Almaras model lags behind the experiments by about 15% and performs best within the selected models, while the $k-\varepsilon$ model shows a very slow rate of dissipation and a slightly higher error. However, the deviation among models is about 3%. For the medium level of $T_i = 1.13\%$, the numerical results of all models follow the experiments

very closely. It can be concluded that, in the free-stream, as the turbulence intensity level rises, the accuracy of Eddy Viscosity Models declines.

The augmented turbulence intensity finally finds its way into the boundary layer and affects the velocity profile and apparent shear stresses. Comparing it to the Musker line as a reference, for the medium level T_i, the experiments measure u^+ higher than the Musker line. However, by increasingRe_x, u^+ approaches closer to the Musker line. On the numerical side, the Spalart-Almaras model follows the Musker line identically, while the $k-\varepsilon$ model and RSM underestimate the u^+ by about -30%. The $SST\ k-\omega$ model follows the same trend as the experiments for the high Reynolds numbers.
When the turbulence intensity is elevated to the high level of $T_i > 5\%$, the experimental results for $u^+ - Y^+$bond to each other as the Reynolds number increases. The Spalart-Almaras model is again in strong agreement with the experiments. The $k-\varepsilon$ and RSM models underestimate the of variation u^+ by about a -30% error and the $SST\ k-\omega$ model identically follows the experiments.

According to the experiments, the apparent shear stresses inside the boundary layer decrease as the Reynolds number increases. This conclusion is not true for the numerical evaluations. For the medium level of T_i, the variation of the Reynolds numbers have only a little affects on the variation of shear stresses. With the $k-\varepsilon$ model, the turbulent shear stresses are predicted nearly constantly between $8 < Y^+ < 120$ and this model is in error qualitatively and numerically by about 25% to 55%. The $SST\ k-\omega$ and RSM models perform better. By approaching to the wall, the RSM has a bit less errors than the $SST\ k-\omega$model.

For high turbulence intensity, the experimental values of apparent shear stresses reduce to about 50% of the previous set of values. The $k-\varepsilon$ model is not affected by the elevation of the turbulence level and performs as it did for the medium level of T_i. Therefore, even serious changes of the turbulence level in free-stream have only a small impact on the shear estimation of the standard $k-\varepsilon$ model. The same conclusion can be made for the RSM. However, the $SST\ k-\omega$ model is affected by the high turbulence intensity of the free-stream, by which the turbulence shear stress is reduced by about 50%. In this case, the error remains at about 60% compared to that of the experiments.

Examining the selected EVMs indicates that:

1. Models are poor in estimating the decay of the high turbulence level flow in the free-stream.
2. Models are successful at predicting the decay of the medium level turbulence in the free-stream.
3. The $SST\ k-\omega$ and Spalart-Almaras models predictions of the variation of $u^+ - Y^+$are satisfactory, while those of the RSM and standard $k-\varepsilon$ models are in serious error.
4. Variation of $u^+ - Y^+$for the high T_i is more accurately predicted by the $SST\ k-\omega$ and Spalart-Almaras models. The RSM and standard $k-\varepsilon$ models are in serious error.
5. For the medium values of T_i, all turbulence models failed to predict within an acceptable range of error the turbulent shear stresses inside the boundary layer. The evaluations of all models are in serious error compared to those of the experiments.

For the high , the standard k model shows no appreciable effect compared to that shown for the medium level of turbulence. A better estimation is provided by the RSM. The $SST\ k$ model follows the same trend as observed in the experiments. However, it stands in serious error when compared to the experiments.

ACKNOWLEDGEMENTS

The authors wish to express their gratitude to the Faculty of Engineering, Ferdowsi University of Mashhad, for the financial support provided for this research.

REFERENCES

Biau, D., D. Arnal and O. Vermeersch, (2007). A transition prediction model for boundary layers subjected to free stream turbulence. *Aerospace Science and Technology*, 11(5), 370-375

Choi, J., S. Teng, J. C. Han and F. Ladeinde, (2004). Effect of free-stream turbulence on turbine bladeheat transfer and pressure coefficients in lowReynolds number.*International Journal of Heat and Mass Transfer*,47(14-16)3441–3452

Colella, F., G. Rein, V. Verda and R. Borchiellini (2011). Multiscale modeling of transient flows from fire and ventilation in long tunnels.*Computers & Fluids*, 51(1), 16-29

Davidson, L., (2003). An introduction to turbulence models, *Publication No 97/2, Chalmers University of Technology*, Goteborg, Sweden

Dris, A. and M. W. Johnson, (2004). Transition on concave surfaces. *Proceedings of TURBOEXPO, GT-2004-53352, International Gas Turbine Congress*, Vienna, Austria

Hussaini Y., J. L. Lumley (1996). Simulation and modeling of turbulent flows, *Oxford University Press*

Johnson, M. W. (2003). A receptivity based transition model. *Proceedings of ASME, GT-2003-30873*, Atlanta, Georgia, USA

Menter, F. R. and R. B. Langtry (2004). A correlationbased transition model using local variables, Part I-model formulation.*Proceedings of ASME TURBO EXPO 2004*, GT2004-53452, Vienna, Austria

Redford,J. A. and M.W. Johnson (2004). Predicting transitional separation bubbles.*Proceedings of TURBOEXPO* 2004, GT-2004-53353, 14-17, Vienna, Austria

Robert, G. J. and D.S. Henningson (1999). Evaluation of data from direct numerical simulations of transition due to free-stream turbulence. *Center for Turbulence Research, Annual Research Briefs*, Report No 205

Rumsey, C. L. and P.R. Spalart (2009). Turbulence model behavior in low Reynolds number regions of aerodynamics flow fields. *AIAA Journal*, 47(4), 1308-1319.

Schaffrath, A., K.C. Fischer, T. Hahm and T. Wussow (2007). Validation of the CFD code fluent by post-test calculation of a density-driven ROCOM experiment. *Journal of Nuclear Engineering and Design*, 237(15-17), 1899-1908

Schlechting, H., (2000). *Boundary layer theory.8th Edition*, ISBN 3-540-66270-7, Springer-Verlag

Sohn, K. H., E.E. Reshotko (1991). Experimental study of boundary layer transition with elevated free-stream turbulence on a heated flat plate. *Report No 187068, Lewis Research Center*. Under Contract NAG3-230, NASA Contractor Report 187068

Spalart, P. R., and S. R. Allmaras, (1994). A one-Equation turbulence model for aerodynamic flows. *La Recherche Aerospatiale*, 1, 5-21

Stefes,B. and H.H. Fernholz (2004). The influence of high free-stream turbulence and a favorable pressure gradient on an incompressible axisymmetric turbulent boundary layer. *European Journal of Mechanics B/Fluids*, 167–187

Wissink, J.G. and W. Rodi (2011). Heat transfer from the stagnation area of a heated cylinder at Re_D=140000 affected by free-stream turbulence. *International Journal of Heat and Mass Transfer*, 54(11-12), 2535-2541

Wang, X. and W. Sun(2011). Effects of non-Uniform inlet boundary conditions and lift force on prediction of phase distribution in upwind bubbly flows with Fluent-IATE. *Nuclear Engineering and Design*, 241(7), 2500-2507

Yang, Z. and I.E. Abdalla (2009). Effect of free-stream turbulence on a transitional separated-reattached flow over a flat plate with a sharp leading edge. *International Journal of Heat and Fluid Flow*, 30(5), 1026-1035

Zhang, J. and E. Morishita E. An efficient and accurate way of posing inflow profile boundary conditions",*The University of Tokyo*, 7-3-1, Hongo, Bunkyo-ku, Tokyo, morisita@meyer.t.u-tokyo.ac.jp